A SYSTEMS ENGINEERING APPROACH TO ELECTRO-MECHANICAL ACTUATOR DIAGNOSTIC AND PROGNOSTIC DEVELOPMENT

Genna Swerdon
Matthew J. Watson
Sudarshan Bharadwaj
Carl S. Byington
Matthew Smith

Impact Technologies, LLC
State College, PA 16801
814-861-6273
Genna.Swerdon@Impact-Tek.com

Kai Goebel
Edward Balaban

NASA Ames Research Center
Moffett Field, CA 94035
Kai.Goebel@nasa.gov

Abstract: The authors have formulated a comprehensive Systems Engineering approach to Electro-Mechanical Actuator (EMA) Prognostics and Health Management (PHM) system development. The approach implements software tools to integrate simulation-based design principles and dynamic failure mode and effects analysis. It also provides automated failure mode insertion and propagation analysis, PHM algorithm design and verification, full dynamic simulations, code generation, and validation testing. This process aims to produce the appropriate fault detection and prediction algorithms needed for successful development of an EMA PHM system.

As an initial use case, the developed approach was implemented to develop and validate a model-based, virtual sensor software package for landing gear EMA PHM. This effort included creation of a dynamic, component-level system model that can be used to virtually sense parameters, detect degradation, isolate probable root cause, and assess severity. This model is also used as a virtual test bed for performing fault insertion analysis to address algorithm development and experimental prioritization. The developed model was validated using data from a test stand, which was specifically constructed for EMA PHM development. The model-based predictor was then coupled with failure mode diagnostics, advanced knowledge fusion, and failure mode progression algorithms to form a complete prototype EMA PHM solution.

Key words: Electro-mechanical actuator (EMA); integrated vehicle health management; prognostics and health management; simulation models; systems engineering; diagnostics; prognostics.

Introduction: Electro-Mechanical Actuator (EMA) systems, which generate controlled linear or rotational motion using a DC motor connected to a ball-screw or gear train, are currently employed in a wide variety of industries, including commercial aircraft, military air/land vehicles, robotics, and industrial process control. In recent years, EMAs have been adapted to many applications where conventional hydraulic actuators have been used previously. Growing interest in power-by-wire aircraft design philosophy is expected to further increase the number of EMA units in military and commercial aircraft applications. The weight reduction, maintenance advantages, and other appealing characteristics of power-by-wire have led to many research and development efforts aimed at expanding the role of EMAs in both military and commercial aircraft applications.[1],[2] Expanded deployment of EMA systems in critical applications has created much interest in Prognostics and Health Management (PHM) of these actuators to ensure reliable and economical system performance, especially in safety-critical applications such as aircraft control. Development of diagnostic and prognostic technologies is therefore needed to enable successful deployment of EMAs in these new applications.

Conventional actuator maintenance procedures often rely on time-based service or replacement of fielded units. This approach, in the worst case, can result in loss of aircraft due to failure occurring before the end of the estimated component life span. However, since component life is generally estimated in a conservative manner to avoid catastrophic failure, maintenance actions are often performed when not warranted by the actual condition. Modern health monitoring techniques that provide an accurate diagnostic assessment of the current component health enable a transition to Condition-Based Maintenance (CBM) where decisions to service or replace components are made according to the current estimated health state.

Prognostic Health Management (PHM) systems go beyond purely diagnostic approaches by estimating the progression of component degradation, thereby generating a continuously updated prediction of remaining component life. This offers additional benefits beyond purely diagnostic systems by allowing advanced scheduling of maintenance procedures, proactive replacement part allocation, and enhanced fleet deployment decisions based upon the estimated progression of component life usage. Prior studies have demonstrated the process of applying PHM techniques to aircraft hydraulic actuator systems and the resulting benefits. [3],[4],[5],[6] As the role of EMAs in aircraft applications continue to increase, PHM technologies will be a vital part of the Condition-Based Maintenance strategy.

In order to facilitate this development, the authors have formulated a comprehensive Systems Engineering approach that consists of a step-by-step process to develop an EMA PHM system. The end result of this process is the appropriate fault detection and prediction algorithms needed for successful EMA PHM. This approach also enables the formulation of a PHM system that can be integrated within the broader Integrated Vehicle Health Management (IVHM) architecture for the entire vehicle. As an initial use case, the developed approach was implemented to develop and validate a model-based, virtual sensor software package for landing gear EMA PHM systems. This effort included creation of a detailed dynamic, component-level model of the system (built in a transportable simulation environment) that can be used to virtually sense parameters and detect degradation, isolate probable root cause, and assess severity. This simulation environment can also be used as a virtual test bed for performing fault insertion analysis to address algorithm development and experimental prioritization. The authors have also designed and constructed an EMA test stand with an extensive sensor suite, including high-performance displacement sensors, accelerometers, thermocouples, and load measurement that provides a comprehensive assessment of EMA response and health state. Data obtained from this test stand has been used to tune and validate the simulation models. Uncertainty assessment methods and model order reduction techniques are also being evaluated with respect to technical accuracy, required processing, and potential effects on safety and life-cycle cost drivers. The model-based predictor, when coupled with failure mode diagnostics, advanced knowledge fusion, and failure mode progression algorithms within a probabilistic framework, forms a complete prototype EMA PHM solution.

Systems Engineering: In order to facilitate the development of EMA PHM, the authors have formulated a comprehensive Systems Engineering approach that consists of a step-by-step process to develop an EMA PHM system. The developed approach uses software tools (FMECA++™ and PHM Design™) developed by the authors that allow for the integration of simulation-based design principles and dynamic failure mode and effects analysis. The integration of these tools provides: 1) automated failure mode insertion and propagation analysis; 2) PHM algorithm design and verification; 3) full dynamic simulations; 4) code generation; and 5) validation testing.

Traditional Failure Modes, Effects, and Criticality Analyses (FMECAs) are commonly used to assess the relative criticality of individual failure modes based on symptoms, failure rates, and subsequent detrimental effects, allowing those with higher risk levels to be eliminated in early stages of system development. Impact has expanded this concept to incorporate PHM considerations, such as sensors and algorithms needed to detect a given symptom and isolate probable root cause, with FMECA++™. Other metrics such as detection and false alarm probabilities, along with detectability and predictability scores, allow a complete relative assessment of fault coverage. Information from a number of typical EMAs was consolidated to create a FMECA++™ for a general EMA.

This information was then modeled using PHM Design™, a software tool that allows the user to design, develop, evaluate, and implement a cost-effective PHM system. In addition to a functional model, which consists of functional areas and either mechanical, electrical, or fluid connections, the software provides a canvas to combine elements typically contained in "paper-based" FMECAs, such as failure modes, symptoms, and effects, with PHM design information such as sensors, algorithms (BIT, diagnostic and prognostic), and maintenance tasks. The software organizes the PHM information, performs metric-based analyses, and enables trade studies to answer difficult PHM or CBM design and development questions. Analysis options are also built-in to provide coverage metrics that help to ensure an optimal PHM solution. These analyses include Criticality, Reliability, Reachability, Diagnosability, and Prognostic Coverage analyses for each failure mode and line replaceable unit (LRU) (Figure 1).

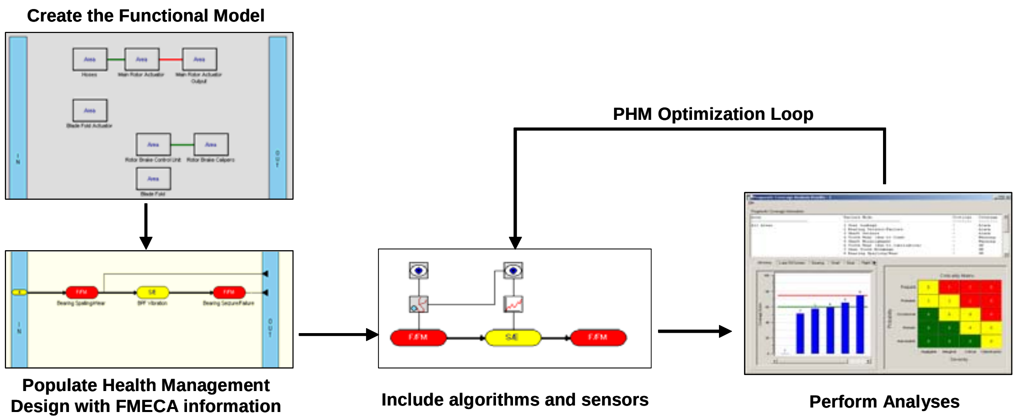

Figure 1 – PHM Design^{TM} Modeling Process

<u>Functional Model and Health Management Design:</u> The PHM Design™ software allows the user to define a functional model of the system that serves to organize the design of the PHM system. Within each functional element, the user can design the Health Management scheme using information from the FMECA++™, as well as expertise and experience. A snapshot of the developed Functional Model and Health Management Design for the target EMA is shown in Figure 2.

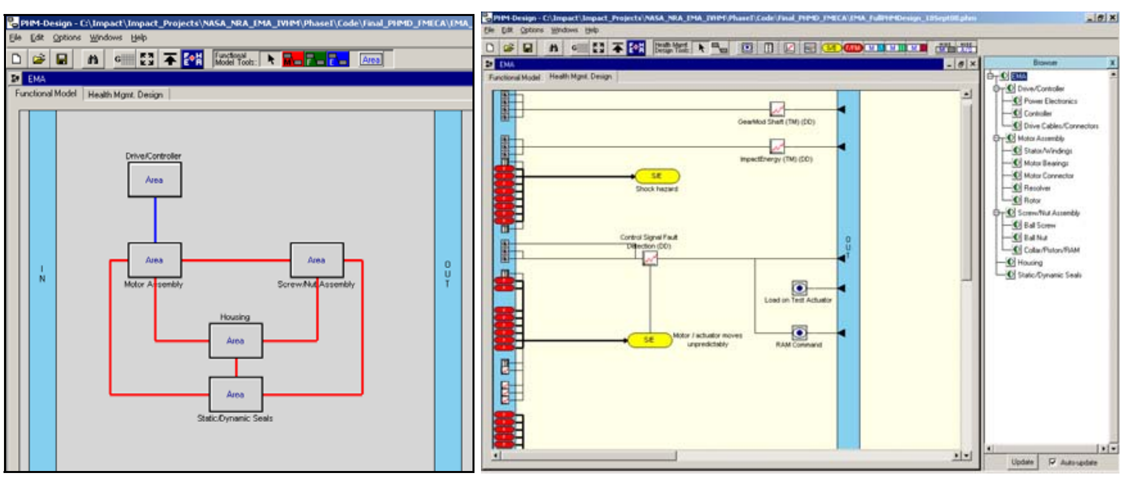

Figure 2 – EMA Functional Model (left) and Health Management Design (right) from Impact's PHM Design™ Software

<u>Criticality Analysis:</u> The Criticality Analysis generates a criticality matrix, which is a popular logistics tool that sorts failure modes in two dimensions by weighing their failure rates and severities. Severity is a failure mode attribute, defined as a number between 1 and 4 for each fault block in the model. Failure rate must also be defined for each failure mode and is categorized at the time of the analyses according to user-defined limits. The most important conclusion the user takes from this analysis is which failure modes fall into the high risk category and should be compensated for with adequate PHM coverage.

<u>Reliability Analysis:</u> The reliability analysis has a very similar objective to the criticality analysis, except it pertains more to fault paths than to individual components. Each failure mode's reliability is calculated based on a reliability equation, which algebraically

combines the reliabilities of multiple failure modes that lie on the same path. The results are organized by the block where the root failure mode appears and may be displayed with respect to time in both tabular and graphical formats (see Figure 3). By viewing all fault reliabilities together, the user can more clearly see which faults paths have the highest risk and would benefit most from the failure risk reduction that PHM offers.

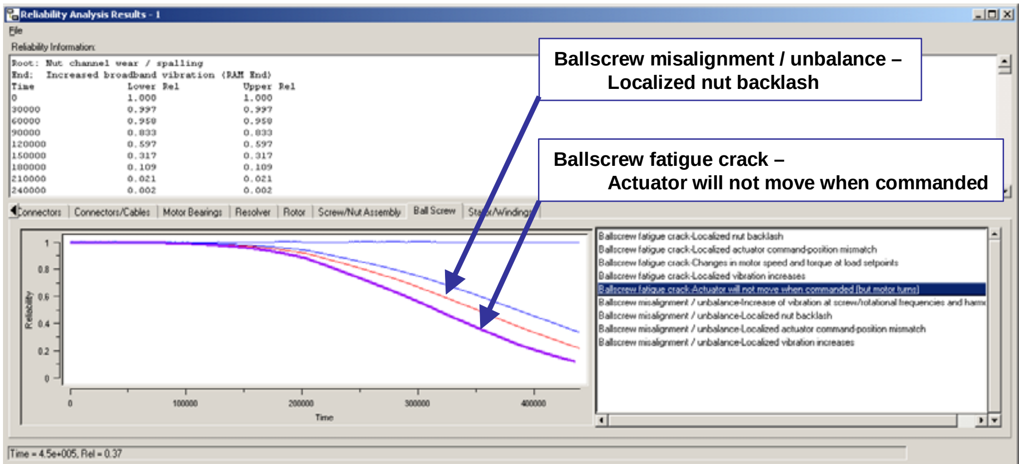

Figure 3 – Example Reliability Analysis

Reachability Analysis: Once the high-risk failure modes are identified, the reachability of each mode is assessed. This analysis identifies all sensors, algorithms, failure modes, symptoms, and maintenance tasks in any way linked to the given component. The output is divided into upstream and downstream elements to give an indication of available diagnostics opportunities. This analysis can also be run on symptoms if the user was more interested in what could cause or be caused by a certain system behavior.

Diagnosability Analysis: Once the model is populated with sensors and algorithms, a diagnosability analysis can be run to evaluate the theoretical performance of the PHM approach. Specifically, it calculates how well a combination of symptoms isolates the root cause to a particular failure mode or line replaceable unit (LRU). Ideally, all failure modes would have some distinctive characteristic that enables a unique identification. However, most times, a single symptom can be caused by multiple faults. The list of potential faults for a given symptom, called an ambiguity group, is included in the top screen of the results (see Figure 4). The bar chart on the bottom is a graphical breakdown of failure mode and LRU isolation. Elements that do not isolate well indicate the need for additional symptoms, sensors, or algorithms to improve their diagnosability.

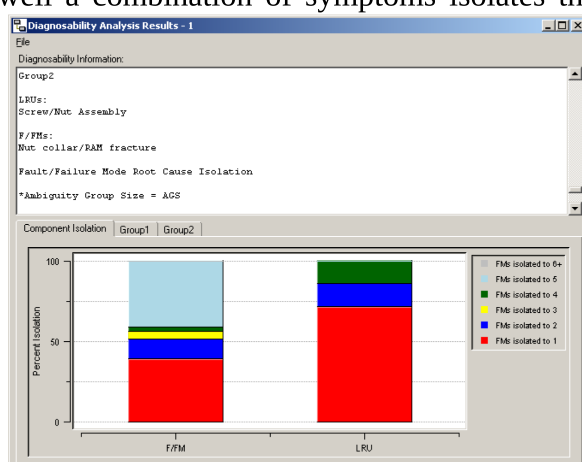

Figure 4 – Example Diagnosability Analysis

<u>Prognostic Coverage Analysis:</u> The prognostic coverage analysis enables the user to realize a system's ability to prevent critical failure modes by effective diagnosis of upstream events. This is done by evaluating the presence and attributes of algorithms along potential causal paths leading to any particular failure mode. The prognostic coverage output is divided into three sections. In the first section, failure modes are sorted by area, based on whether they are safety or flight critical ("sc" or "fc") and their coverage condition (ok, warning, or alarm). This classification is determined from the prognostic coverage value and the location in the criticality matrix since the level of coverage required to be considered adequate is set higher for critical faults than it is for less critical faults. The "alarm" condition will only be assigned if the failure mode is in the medium or high risk regions. The second section indicates the prognostic coverage values sorted from least to most coverage. The third section, the criticality matrix, shows a quick reference of the failure mode locations. Each cell of the matrix lists all failure modes belonging to that combination of probability of occurrence and severity.

Based on the results of the PHM Design™ model, certain faults and failure modes have been identified as high risk (see Figure 5), while certain others were tagged as low risk and thus eliminated from consideration.

Failure Mode	Risk
Motor bearing wear / spall	High
Motor bearing lubrication degradation	High
Nut channel wear / spalling	High
Nut looseness / slipping	High
Motor shaft eccentricity	High
Motor winding shorted/open	High
Seized motor bearing / shaft	High
Loss of Power	High
Nut cracked / **fractured**	High
Resolver fault **/ failure**	High
Ballscrew/nut jammed/seized	High
Ballscrew fracture	High

*Functional failures in bold

Failure Mode	Risk
Power transients	Medium
Ballscrew wear / spalling	Medium
Ballscrew fatigue crack	Medium
Screw/nut lube degradation	Medium
No signals generated	Medium
Nut collar/RAM fracture	Medium
Seal Degradation	Medium

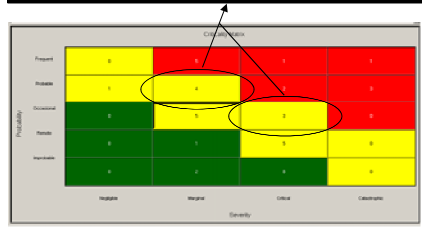

Figure 5 – Failure Mode Candidates from PHM Design™ Criticality Analysis

Model-Based PHM: The model-based approach to PHM (Figure 6) applies physical modeling and advanced parametric identification techniques. As an advantage over 'black-box' or purely data-driven health-monitoring schemes, faults and failure modes are traced back to physically meaningful system parameters providing the maintainer with invaluable diagnostic information. The approach employs a mathematical dynamic model of the system that is directly tied to the physical processes that drive the health of the component. The control command is used on the model to simulate expected system response. The difference between the simulated and actual response is used to perform an estimation of system parameters (e.g., efficiency, friction factors, etc.). The estimated parameters are then compared with the baseline health level parameters to identify and isolate system faults and provide a measure of fault severity.

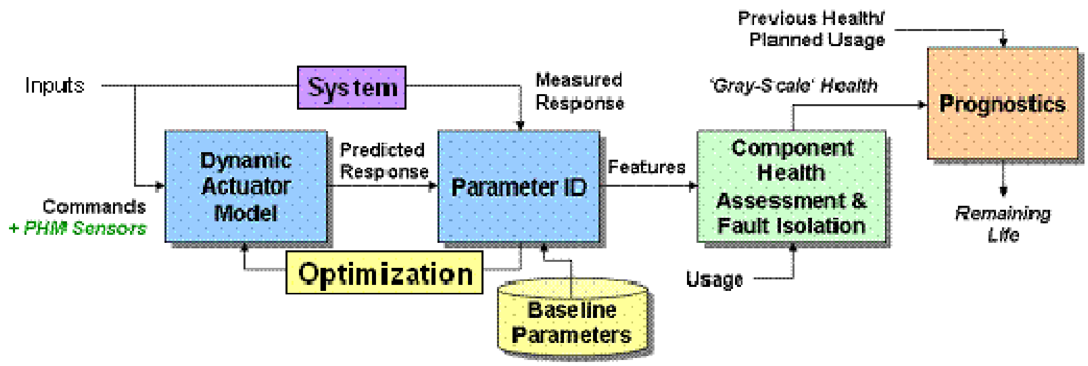

Figure 6 – Model-Based PHM Approach

A generalized dynamic system model of electro-mechanical actuators was developed to aid in the refinement of model-based PHM techniques for EMAs. This model was created in the Simulink® environment of the MATLAB® software package and can be employed to represent the physics of system degradation and its effects on the performance of components or subsystems within the overall actuator system. A virtual test bed application was developed to exercise this model under a variety of baseline and faulted conditions. The following sections detail these development efforts.

Dynamic System Model Development: A schematic of the general EMA system represented by the model is shown in Figure 7, while the developed EMA Simulink® model is shown in Figure 8.

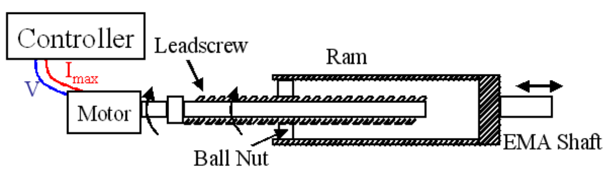

Figure 7 – Schematic of Electromechanical Actuator

The model incorporates blocks for the various components within the EMA, such as the brushless DC motor, leadscrew and ball nut, ram, and output shaft. It also contains blocks for components such as the gearbox and encoder, which can be selected or deselected by the user, since these components may not be present on all EMAs. Similarly, the user may also select the type of control for the EMA with the available choices being position control, velocity control, or torque control. In addition, the model incorporates fault blocks within the various components. These blocks insert faults by modifying the control or feedback signals, or characteristic parameters within the component. Also, faults may be simulated by introducing biases or noise into actuator commands or measured responses.

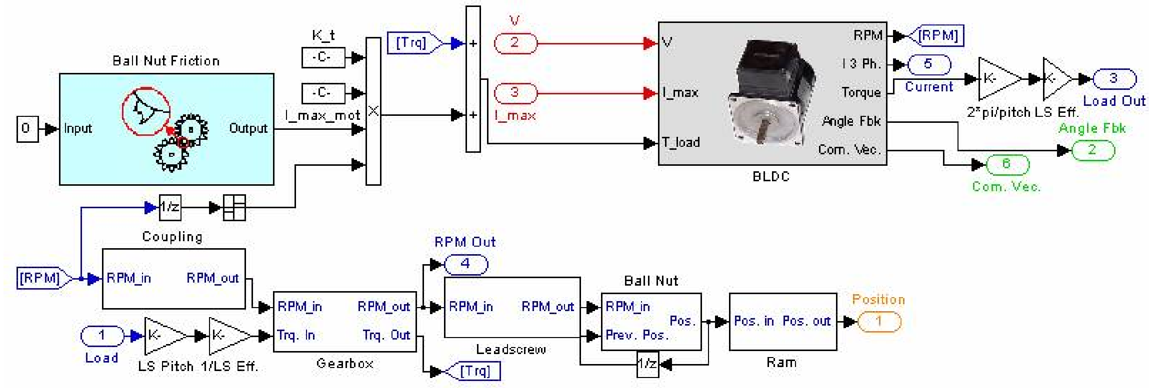

Figure 8 – Dynamic Model of Generalized EMA System

The major assumptions made in creating this EMA model are listed below.

1. Three phase brushless DC motor drives leadscrew
2. Each phase of motor is modeled as L-R circuit
3. Leadscrew, ball-nut, and ram modeled as rigid components with mechanical efficiencies
4. Shaft angular acceleration is proportional to excess torque (motor torque, less damping and load torques)
5. The motor is governed by the relationships shown in Eq. (1) to (3):

$$I_\phi = \frac{V_\phi}{R_\phi + L_\phi s} \tag{1}$$

$$\tau_\phi = k_{t_\phi} I_\phi \tag{2}$$

$$\tau_{Total} = J\ddot{\theta} + B\dot{\theta} + \tau_l \tag{3}$$

where I_ϕ is the current in each phase, V_ϕ is the voltage in each phase, R_ϕ is the winding resistance in each phase, L_ϕ is the winding inductance in each phase, τ is the motor torque, k_t is the torque constant, J is the rotor inertia, B is the damping on the rotor, and τ_l is the load torque acting on the rotor shaft.

In addition to modeling the electrical and mechanical parts of the EMA, a thermal model of the EMA motor was implemented. As Figure 9 shows, the model treats the motor windings as a lumped system and determines their temperature at each time step based on the input heat (I^2R losses) and the heat lost to the surface of the motor. The motor surface then loses heat to the ambient air through convection and gray-body radiation.

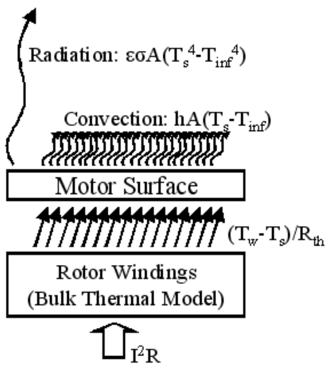

$$\left(I^2R - \frac{T_{w,i-1} - T_s}{R_{th}}\right)dt = m_w C_{pw}(T_{w,i} - T_{w,i-1})$$

$$\frac{T_{w,i-1} - T_s}{R_{th}} = hA(T_s - T_{\inf}) + \varepsilon\sigma A\left(T_s^4 - T_{\inf}^4\right)$$

I	:	Winding Current	σ	:	Stefan's Constant
R	:	Winding Resistance	ε	:	Surface Emissivity
R_{th}	:	Thermal Resistance	T_s	:	Motor Surface Temperature
dt	:	Simulation Time Step	T_{inf}	:	Ambient Temperature
m_w	:	Mass of Windings	$T_{w,i-1}$	:	Winding Temperature at Timestep i-1
C_{pw}	:	Specific Heat of Windings			
h	:	Heat Transfer Coefficient	$T_{w,i}$	:	Winding Temperature at Timestep i
A	:	Motor Surface Area			

Figure 9 – Thermal Model of Actuator Motor

Virtual Test Bed Development: A Virtual Test Bed Environment (VTBE) was developed (also in Simulink®) to allow simulation of the developed model, critical faults, and other external effects (i.e., loads, control inputs, etc) that contribute to prediction uncertainty. This environment can be used to execute the validated model with various healthy and simulated fault conditions to produce a database of model parameters that characterize the response of the system.

For initial demonstrations, the VTBE is based on an EMA Test Stand constructed by the authors. The physical test stand includes components to subject the test actuator to the desired load profiles, as well as to generate the control profiles that define actuator motion. The test rig also incorporates a variety of sensors to obtain and characterize the response of the actuator system to various external stimuli. These additional elements of the test rig are therefore also modeled in the VTBE, so as to subject the actuator model, in the digital realm, to the required excitation profiles and loading conditions. The VTBE consists of a loading system, a controller, an actuator drive, and the required sensor blocks. Since the loading system was modeled as another EMA opposing the test EMA, an additional drive was also modeled for the load actuator. A block diagram of this test bed environment, showing the various control modes and feedback loops, is shown in Figure 10.

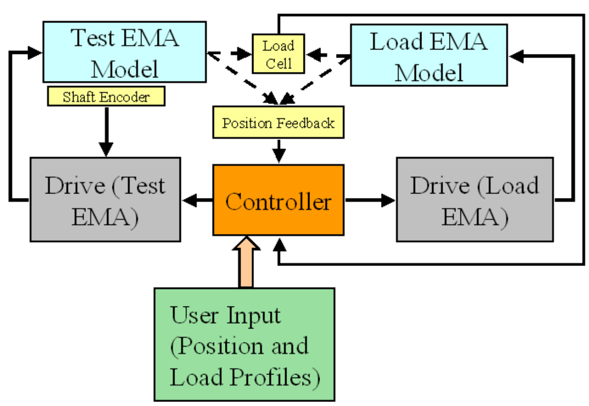

Figure 10 – Block Diagram of Virtual Test Bed Environment

As seen from the figure, a master controller sends command signals to the test and load

EMA control drives. The drives command the respective EMA voltage and current levels. The master controller receives feedback from the position sensor and sends a control signal to the test EMA drive to correct for the position error. The controller also receives a load feedback signal from the load cell between the EMA shafts. The controller sends a signal to the load drive to minimize the load response error. A diagram of the actuator model within the Virtual Test Bed Environment is shown in Figure 11.

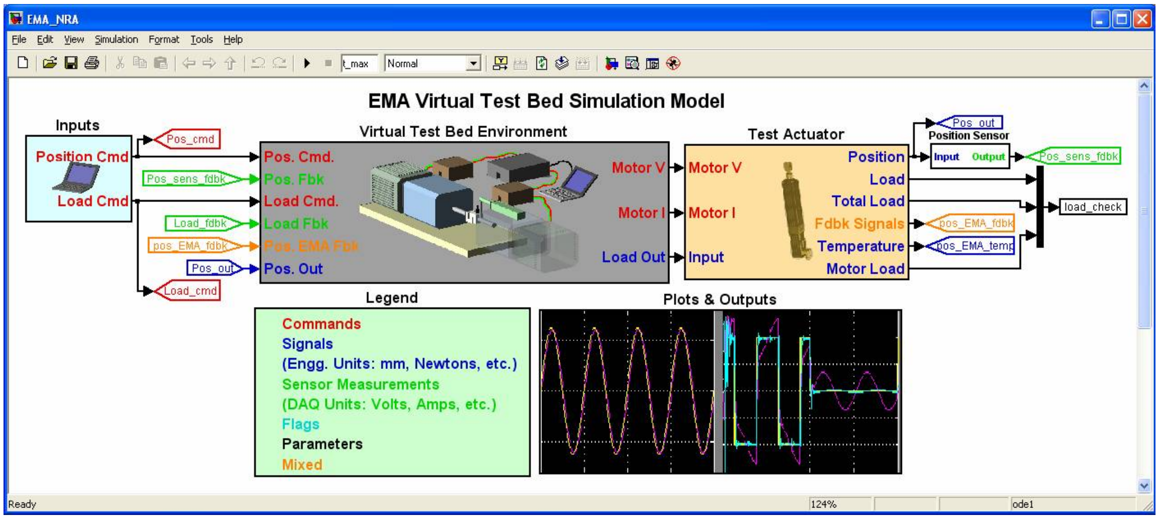

Figure 11 – Simulink® Virtual Test Bed Environment

Simulations performed by the authors initially consisted of observation of the system response to various position and load profiles under expected healthy conditions. For instance, Figure 12 shows the response of the test EMA to a sinusoidal position profile with a step change in the load. As seen, the controller and drive are able to maintain the specified position profile (top left plot) against the jump in the load. The bottom left plot shows a step change in the current drawn corresponding to the change in the load (top right plot). The bottom right plot shows the temperature of the EMA motor windings and surface. As expected, the higher current draw from t=20 seconds causes a faster rise in both temperatures.

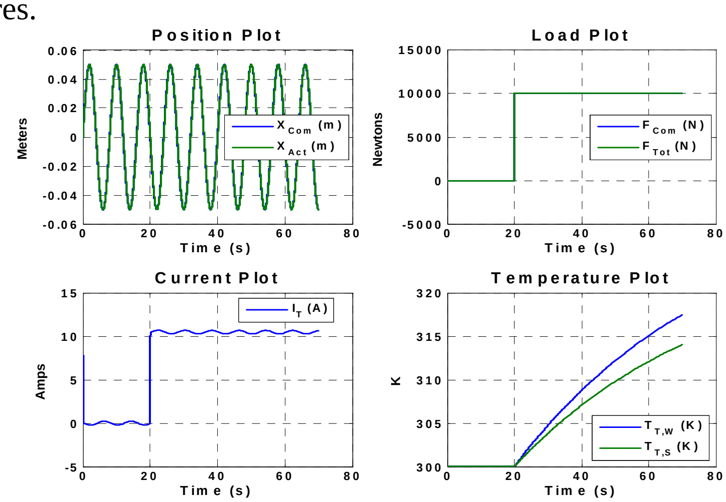

Figure 12 – EMA Model Response to Sine Position and Step Load Profiles

Similarly, the response of the EMA to other command profiles was evaluated, and the ability of the controller to maintain the required position and load profiles was verified. The response signals of the EMA (such as RPM, temperature, etc.) were analyzed as checks on the EMA operation.

The model and VTBE were then used to conduct fault simulation tests. Faults were modeled as gain, bias, and/or noise blocks on various parameters and signals. For example, Figure 13 shows the simulation of a “loss of power to the motor” fault (see the left half of the figure). This fault is simulated by specifying a gain of zero on the motor command (with no bias or noise). The right half of the figure shows the EMA response to a sinusoidal position profile with a steady load ramp under the influence of this fault. As seen, the system is initially able to follow the position command (top left plot in right half of the figure). When motor power is lost, the test EMA goes dead. However, the load EMA exerts a steady load according to the specified load profile, causing the test EMA shaft to retract. As the bottom left plot in the right half of the figure shows, there is still current in the test EMA windings. This current is induced by the back EMF generated by the motion of the shaft, which forces the motor to turn despite the loss of power. Once the power is turned back on, the system resumes normal operation.

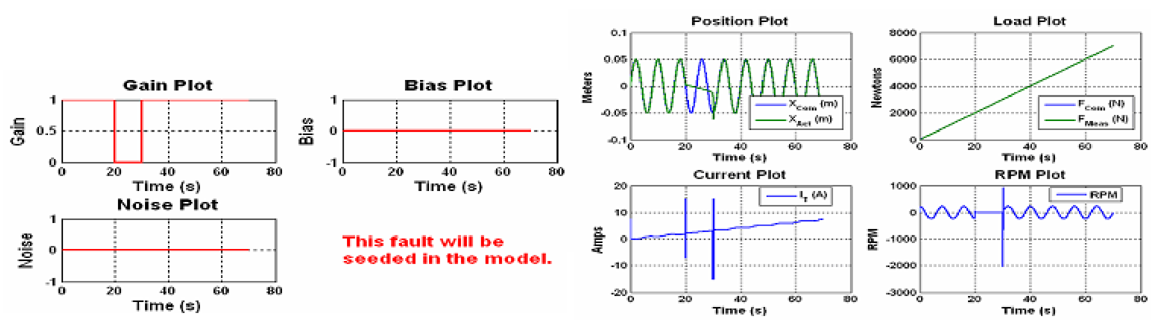

Figure 13 – EMA Response to Power Loss Fault

Similarly, a winding short was simulated in the motor (Figure 14). This was achieved by using a gain block to reduce the “number of winding turns” parameter (see left half of the figure). The winding short was simulated in two phases: an initial mild fault, followed by a deteriorating fault that slowly recovers. The right half of the figure shows the system response to a sinusoidal position profile and rectangular load profile. As the bottom left plot in the right half of the figure shows, the initial mild winding short causes a rise in the motor current, which compensates for the reduced torque constant (owing to the reduced effective number of windings). Thus, the actuator is still able to follow the specified position profile (top left plot in the right half of the figure). However, the maximum current that the motor can draw is limited by the drive. This limits the compensation that the motor can provide against the later deteriorating fault, causing the shaft to deviate from the position command. Once the fault is removed, normal motion resumes.

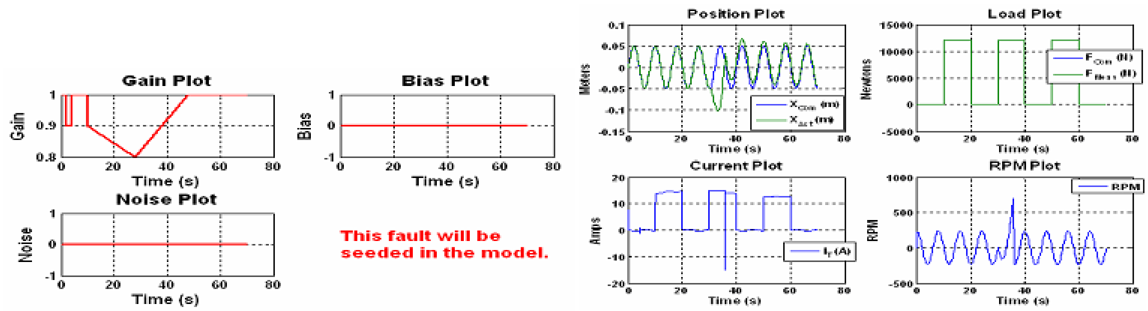

Figure 14 – EMA Response to Winding Short Fault

<u>Preliminary Model-Based PHM Results:</u> The authors have also developed preliminary fault assessment routines to detect and assess the severity of faults that were simulated in the dynamic actuator model. These routines implement a reduced order (static) actuator model, derived from an order-reduction analysis performed on the full dynamic model. The routines also incorporated an automated optimization routine to obtain model parameters, based on error minimization between dynamic model responses to command signals and the reduced order model responses to the same signal. In this sense, the dynamic model was used to mimic an actual (physical) EMA, in that the responses from the dynamic model are used to represent the actual response of the system. As described above, the Virtual Test Bed Environment was used to simulate three EMA faults, which were identified from the systems engineering analysis using PHM design™. These faults were:

- Motor phase 1 winding short
- Motor bearing wear/lubrication degradation (increased bearing friction)
- Position sensor fault

Using the developed PHM approach, the model parameters needed to minimize error were then used to predict fault severity levels for each simulated fault. For example, the effective number of motor windings was used to predict the severity of the winding short fault (Figure 15). Not only did this provide an accurate estimate of fault severity during more severe fault levels, it also performed well for moderate fault levels. As seen in the figure, even though the initial fault does not cause any significant deviation of the measured position from the commanded position, the PHM algorithm is still able to estimate the severity of the fault. It is also worth noting that the deteriorating winding short caused current limiting circuitry within the drive to enter the picture, which is why the position response of the EMA is affected (at roughly 30 sec). This initially throws off the diagnostic feature, but fault estimation accuracy subsequently recovers.

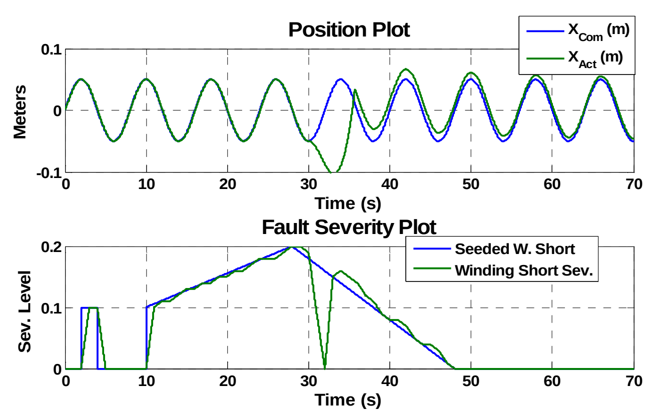

Figure 15 – Diagnosis of Winding Shorts

Similarly, motor bearing wear can be diagnosed using the "bearing friction" parameter. This friction is simulated as an excess torque that the motor has to overcome and is specified as a fraction of the motor's total torque capacity. Figure 16 shows that the bearing friction parameter is able to reliably assess the level of wear in the EMA motor bearings.

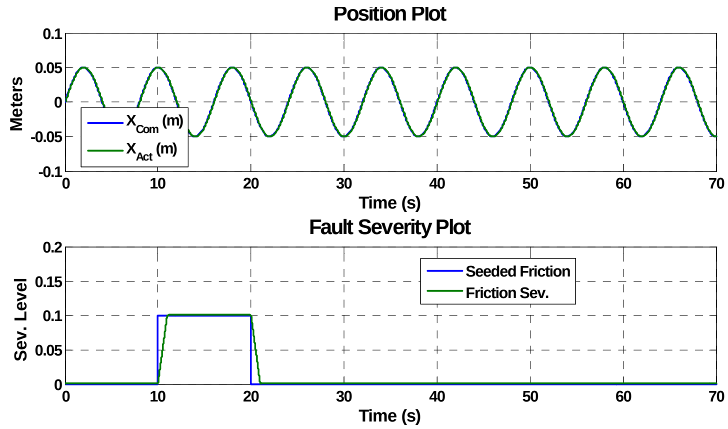

Figure 16 – Diagnosis of Bearing Wear (Friction)

Fault separability was also assessed by simulating multiple faults in the system and observing the response of the developed algorithms. For example, Figure 17 shows the simulation of three faults simultaneously: winding shorts, bearing wear, and position sensor malfunction. As seen, the developed PHM system is able to reliably separate these faults for the most part, with brief inaccuracies manifesting themselves when the level of the simulated fault abruptly changes. An example of this transient effect can be observed as spikes in the winding short and friction severity values at t~30 seconds, when the LVDT fault is removed.

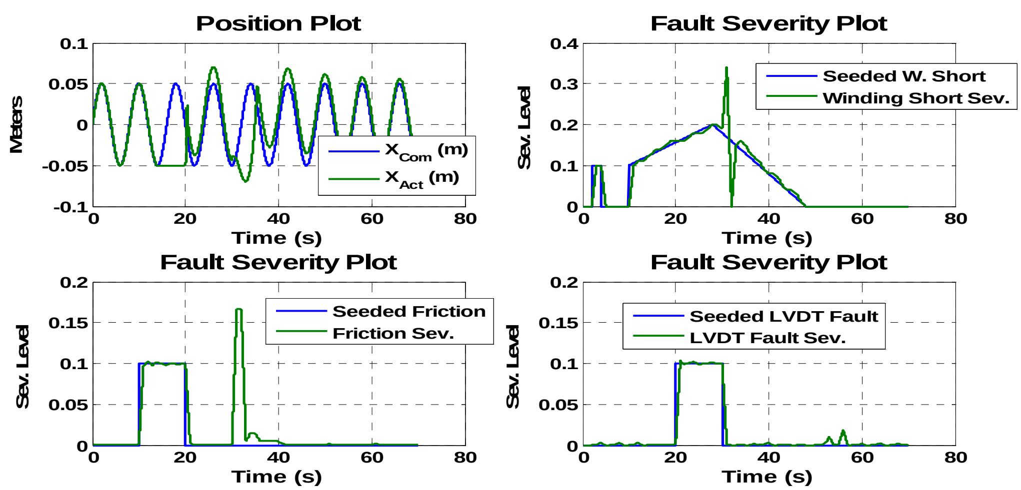

Figure 17 – Diagnosis of Multiple Faults

Conclusions: The authors have developed a Systems Engineering approach that consists of a step-by-step process to develop an EMA PHM system. As an initial use case, a model-based EMA PHM system was also developed using the developed methodology. Preliminary fault assessment routines, based on an initial reduced-order model of the dynamic EMA model, have been shown to perform well for a subset of the faults derived from the systems analysis.

The end goal of the effort is to develop advanced fault diagnostics and prognostics routines for the primary failure modes of interest in EMA systems. The developed techniques are expected to enhance PHM value for EMA systems, and thus increase system reliability and mitigate the effects of catastrophic EMA failures in true power-by-wire aircraft systems. Ultimately, the software will be adaptable and applicable to hydraulic, electro-hydraulic, and electro-mechanical actuator systems and implemented as an on-board, at-wing, or overhaul-level maintenance strategy. The realization of such an automated, prognostic reasoning package will significantly enhance the ability to safely operate the aircraft, schedule maintenance activities, optimize operational life cycles, and reduce support costs.

Future Work: A number of tasks remain to be performed with the EMA PHM development effort. Initially, the accuracy of the EMA model and the Virtual Test Bed Environment will be enhanced using test stand data. Tuning of the parameters of the model is an additional task in this regard, and will be performed with experimental data collected from the test stand. Additional fault scenarios will also be investigated and simulated in the model or through seeded fault testing on the test stand. The fidelity of the developed fault classification algorithms will be enhanced to provide more accurate classification. Advanced algorithms will be used to provide incipient fault detection, while extracted features and models will be used for failure progression tracking and remaining useful life (RUL) prediction through complementary prognostic techniques. Fusion will also be readily implemented at various levels, including the sensor-level (fusing of raw data to increase signal characteristics and reduce noise effects), feature-level (fusing of extracted features), and knowledge level (fusing of health assessment results) to improve algorithm performance and confidence. The authors will also implement model order-reduction techniques to reduce the processing needed to implement the developed model-based approach. This process will facilitate implementation on embedded applications, as well as other applications with strict processing limitations. The performance of the reduced model(s) will then be compared with the full approaches to trade technical accuracy, required processing, and potential safety and life-cycle cost drivers.

Finally, the developed approaches will be demonstrated on an experimental EMA test stand. In this test stand (Figure 18), two actuators (test, load) are directly coupled with minimal compliance, though allowing for minor shaft misalignment. A central PC-based interface manages all test definition, system control, data acquisition, and visualization functionality, and also allows simultaneous execution of real-time PHM algorithms. The test EMA is heavily instrumented to provide high fidelity system response measurements, thus allowing enhanced understanding of degraded EMA response.

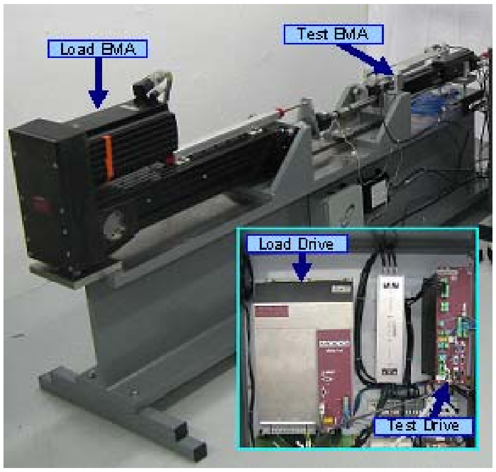

Figure 18 – Test/Load EMAs and Servo Drives (Inset)

Acknowledgments: The work described in this paper was conducted under NASA contract NNA08BA23C. The authors would also like to acknowledge the significant contributions of our colleagues at Impact Technologies, including Michael Ingalls, John Herzog, Sanket Amin, and Greg Kacprzynski, without whom this work would not have been possible.

References:

[1] Jensen, S.C., Jenney, G.D., Dawson, D. “Flight Test Experience with an Electromechanical Actuator on the F-18 Systems Research Aircraft,” IEEE Digital Avionics Systems Conferences, October 7-13, 2000.

[2] Blanding, D.E., “An Assessment of Developing Dual Use Electric Actuation Technologies for Military Aircraft and Commercial Application,” IECEC Energy Conversion Engineering Conference, July 27 – August 1, 1997.

[3] Byington, C.S., Watson, M., Edwards, D., and Stoelting, P., “A Model-Based Approach to Prognostics and Health Management for Flight Control Actuators,” Proc. of the IEEE Aerospace Conference, 2004, Vol. 6, pp. 3551-3562.

[4] Byington, C., Watson, M., and Edwards, D., “Data-Driven Neural Network Methodology to Remaining Life Predictions for Aircraft Actuator Components,” Proc. of the IEEE Aerospace Conference, 2004, Vol. 6, pp. 3581-3589.

[5] Moseler, O., Juricic, D., Rakar, A., Muller, N. “Model-based fault diagnosis of an actuator system driven by the brushless DC motor,” American Control Conference, 1999, Vol. 6, pp. 3779-3783.

[6] Smith, M.J., Bharadwaj, S.P., Swerdon, G.M., Goebel, K., Balaban, E., “Experimental and Analytical Development of Health Management for Electro-Mechanical Actuators,” IEEE Aerospace Conference, to be presented March 2009.